Nanoarchitecture: Toward Quantum-Size Tuning of Superconductivity

*Konstantin Yu. Arutyunov, Vitali V. Zavialov, Egor A. Sedov, Ilia A. Golokolenov, Anastasia A. Zarudneva, Kirill V. Shein, Igor N. Trun'kin, Aleksandr L. Vasiliev, George Konstantinidis, Antonis Stavrinidis, George Stavrinidis, Mihail D. Croitoru, and Arkady A. Shanenko**

Quantum confinement is known to affect a nanosized superconductor through quantum-size variations of the electronic density of states. Here, it is demonstrate that there is another quantum-confinement mechanism overlooked in previous studies. In particular, it is found that the electron–electron attraction can be enhanced due to quantum-confinement modifications of electronic wave functions. The superconducting correlations are strengthened by such quantum mechanical effect, which creates a subtle interplay with surface–substrate phonon modifications. The combined effect depends on nanofilm thickness and can be controlled by nanoarchitechture. The calculations are in a reasonable agreement with experiments performed on high-quality aluminum films. These findings shed light on the long-standing problem of the size dependence of the critical temperature in low-dimensional superconductors.

Nanosized superconductors, in which at least one dimension is of nanoscale, attract significant interest because their properties may vary strongly with system geometry, see, for example, ref. [1]. This opens prospects of architecting superconducting nanostructures in order to improve and even tune their characteristics. The most important of them is the critical temperature T_c.

Main factors that can raise/lower the critical temperature of conventional superconducting materials are well-known since the early years of the BCS theory: modifications of the phonon spectrum[2,3] and disorder effects.[4] Therefore, when first results on the dependence of the critical temperature of nanodimensional superconductors on their geometry appeared, these two factors were immediately employed for explanations; see, for example, refs. [5–7] related to phonon effects and refs. [8–13] dealing with the disorder-driven suppression of superconductivity. However, after in-depth analysis, it became clear that there exists another effect that can significantly influence the physical properties of superconducting nanostructures. This is the quantum confinement of charge carriers.[14–21] At present it is considered that these three mechanisms are mainly responsible for the properties of metallic nanoscale superconductors. One should also keep in mind, of course, impact of fluctuations in systems with critically small dimensions.[1,21]

Though the three basic mechanisms have been figured out, the story is far from being finished. The point is that these mechanisms strongly interfere with one another and their nontrivial interplay depends significantly on structure/morphology of nanosized superconducting systems. Hence, even nowadays interpretation of experimental data still remains a nontrivial task. For example, recent observations of the significant enhancement of T_c in a monolayer of FeSe grown on a SrTiO$_3$ substrate (up to 107 K, as compared to bulk 9 K[22–25]) remains mysterious, though several models have been suggested, see, for example, ref. [26] and references therein. Thus, physicists still continue investigating a plethora of possible options of the complex interplay between quantum-size effects (including those of the superconductor–substrate interface), disorder and phonon physics in order to explain the size

---

Prof. K. Yu. Arutyunov, E. A. Sedov, I. A. Golokolenov, A. A. Zarudneva, K. V. Shein
National Research University Higher School of Economics
Moscow 101000, Russia

Prof. K. Yu. Arutyunov, V. V. Zavialov, I. A. Golokolenov, P. L. Kapitza Institute for Physical Problems RAS
Moscow 119334, Russia

Prof. I. N. Trun'kin, Prof. A. L. Vasiliev
Kurchatov Institute
1 Akademika Kurchatova pl., Moscow 123182, Russia

Prof. A. L. Vasiliev
Institute of Crystallography RAS
Moscow 119333, Russia

Prof. G. Konstantinidis, Prof. A. Stavrinidis, Prof. G. Stavrinidis
Institute of Electronic Structure & Laser (IESL)
Foundation for Research & Technology Hellas (FORTH)
P.O. BOX 1385, Vassilika Vuton, 70013 Heraklion, Greece

Prof. M. D. Croitoru
Institut fur Theoretische Physik III, Bayreuth Universität
95440 Bayreuth, Germany

Prof. A. A. Shanenko
Departamento de F´ısica, Centro de Cîencias Exatas e da Natureza (CCEN)
Universidade Federal de Pernambuco
Av. Prof. Moraes Rego 1235, Cidade Universitária, 50670-901 Recife, PE, Brazil
E-mail: arkadyshanenko@df.ufpe.br

DOI: 10.1002/pssr.201800317

dependence of T_c in nanosized superconductors. To name a few, see, for example, studies on the forward-scattering enhancement of electron-phonon interaction,[26] interfacial coupling between electrons and phonons,[25] the phonon and impurity smearing of the quantum-size peak structure in the electronic density of states (DOS),[27,28] etc.

It is well known that quantum confinement affects the system through variations of the electronic DOS responsible for quantum-size oscillations of the superconducting properties.[14–21] Here we reveal another important quantum-confinement mechanism that is usually overshadowed by the quantum-size variations of DOS and was overlooked in previous studies. In particular, we demonstrate that the electron-electron attraction can be enhanced by quantum-confinement modifications of electron wave functions. Combining experiment and theoretical study of the Bogoliubov-de Gennes equations for high-quality polycrystalline superconducting aluminum nanofilms, we show that T_c is significantly increased as compared to bulk as a result of an interplay between this quantum-mechanical effect and the surface-substrate induced phonon changes. The quantum-size oscillations are washed out due to inevitable fluctuations of the nanofilm thickness in realistic polycrystalline samples studied in experiments.

Experimental Section: Aluminum has been selected as the material where the size dependence of T_c is very pronounced. In early experiments it has been noticed that T_c in aluminum nanofilms is, as a rule, higher than in bulk samples.[29–36] This has been confirmed in numerous experiments. However, differences between various sample sets (material of the substrate, the film deposition rate, the temperature of the substrate while deposition, etc.) resulted in significant variations of the grain size in polycrystalline samples, leading to uncertainties in data and complicating/questioning theoretical interpretations. The objective of the experimental part of this work is to produce and study high-quality polycrystalline aluminum nanofilms with the size of crystallites comparable to the film thickness and fabricated under the same conditions. Notice that in this case the quantum-confinement boundary conditions for electron wave functions at the crystallite surface reduce to those at the film surface, which simplifies the accompanying theoretical analysis.

A set of aluminum nanofilms with thickness d ranging from 5 nm up to 100 nm has been fabricated. The films were e-beam evaporated on single-crystalline GaAs substrate at vacuum 10-9 m*Bar*. High resolution TEM analyses has revealed the expected polycrystalline structure with the average grain size compared to the nanofilm thickness, see **Figure 1**. An amorphous layer of thickness 3 nm is observed at the interface with GaAs substrate, and the native oxide layer of about 2 nm – at the outer boundary. These two imperfections are the main sources of uncertainty in determination of the “true” thickness of the samples. Based on TEM analysis combined with earlier studies on aluminum nanowires[37–40] we may claim that in such ultra-high-vacuum deposited aluminum nanofilms the grain boundaries do not contain any foreign material being just a metal-to-metal interface between two single crystals of different crystallographic orientation. It should be also noted that superconductivity is a rather “rigid” property with respect to foreign impurities. In particular case of aluminum, several atomic percents of ferromagnetic impurities are required to alter significantly the critical temperature.[41] Summarizing, we do not see any channels of inelastic scattering of electrons capable to severely modify the standard BCS electron-phonon mechanism in our samples.

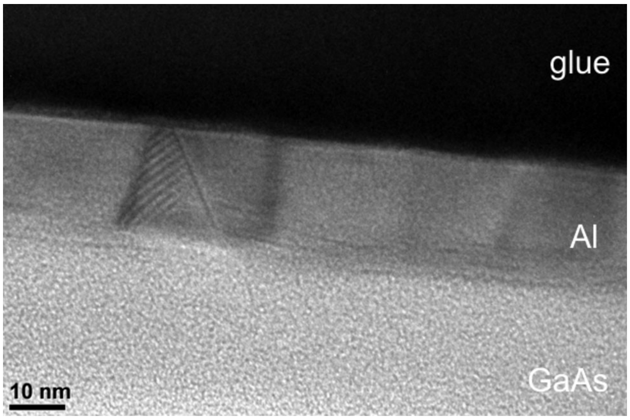

Figure 1. TEM image of a typical polycrystalline aluminum film with nominal thickness 20 nm fabricated by e-gun evaporation in vacuum 10–9 mBar on GaAs substrate. One can distinguish granular structure with the average grain size in all three dimensions being comparable with the film thickness.

Measurements of the aluminum nanofilms were made either in direct-pumped 4He bath with base temperature down to ≈ 1.35K, and in 3He sorption cryostat capable to reach much lower temperatures down to 0.4 K. In both systems the thermometers were calibrated with accuracy ≈ 1 mK against either 4He pressure, or reference points of superconducting transition of extra pure bulk superconductors (tantalum, tin, indium, aluminum, and titanium). The reference point of superconducting transition of bulk 99 9995% pure aluminum $T_c = 1.19$ K corresponds well to literature data. All input/output lines connecting the sample with digital electronics were carefully filtered.[42] The measurements of the sample resistance were made in 4-probe configuration using DC currents of about 0.1 uA, pulse current delta-sigma algorithm and lock-in AC measurements. Within the experimental errors for all samples the increase of bias current up to several uA did not alter the shape of the $R(T)$ transition.

The typical $R(T)$ transition of a 25 nm thick aluminum nanofilm is presented in **Figure 2**. Here by definition, we take the critical temperature T_c as the point where the resistance has dropped by factor of 2 compared to normal state value. The sharpness of the transition enables us to determine the critical temperature with accuracy of about $T_c \approx +/-1$ mK, which is well below the pronounced size effect under the study. The results of the measurements are given by solid circles in **Figure 3**(a). Here we have also added, for illustration, data from some previous studies,[5,30,32,34,36] given by squares, crosses, empty circles, stars, and triangles, respectively. One can clearly notice the general trend: the thinner is the aluminum film, the higher is the critical temperature. The poor quantitative agreement between the previous and our results reflects the difference in fabrication conditions, which can lead to significant variations in the characteristic size of relevant crystallites. The exception is sparse data of refs. [34] and [36], where the latter were measured for samples with strongly coupled and large crystallites. As it has been noted before, T_c of a polycrystalline aluminum nanofilm depends strongly on the sample morphology, for example, on the crystallite (grain) size, see the discussion in ref.[31]. Notice that in Figure 3(a)

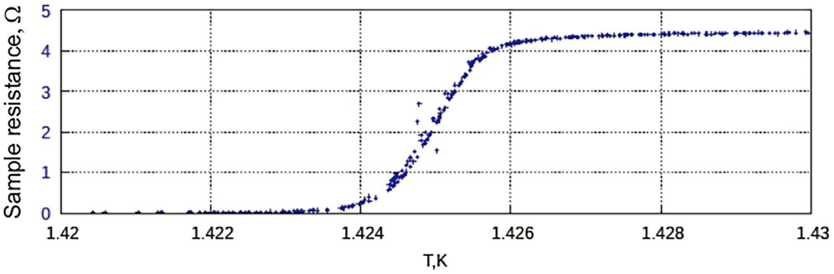

Figure 2. Typical $R(T)$ dependence of the 25 nm thick aluminum film measured with 500 nA excitation current.

we display the previous data-sets with clear dependence of T_c on the nanofilm thickness d rather than measurements for samples with ultrasmall grains whose characteristic size is not in correlation with d, as, for example, refs. [31,33,35]

Theory: We deal with high-quality aluminum nanofilms so that disorder plays a minor role and can be ignored to a first approximation. Thus, we expect that the enhancement of T_c found in our experimental data is controlled by phonon and quantum-confinement effects (see the Introduction).

To take into account the modifications of the phonon spectrum, we keep in mind that our nanofilms are far beyond the ultrathin regime where the surface/substrate contribution plays the major role. In our case such a contribution can be considered as a perturbation, and hence we are able to follow a simple approach developed in a number of previous studies, see refs. [5,6,17,19,20]. Following this approach, one take the effective electron-electron interaction strength in the form of the expansion in powers of 1/d, that is,

$$g = g_0 + \frac{g_1}{k_F d} + \frac{g_2}{(k_F d)^2} + \dots \qquad (1)$$

where g_0 stands for the bulk coupling, $g_i\,(i = 1, 2, \dots)$ are associated with the surface-substrate effects, and k_F is the Fermi wavenumber. Equation (1) is valid for $k_F d \gg 1$ while more complex approach is required for $k_F d \lesssim 1$.

For quantum-confinement effects one needs a more elaborated treatment. Since 1960s it is known that in high-quality nanosized superconductors, T_c (and other superconducting properties) can exhibit oscillations when changing the characteristic dimension(s) of the system.[14–20] For example, in nanofilms the conduction band splits into a series of subbands, and bottoms of such subbands correspond to quantum-well states (QWS) of the confined motion of electrons in the direction perpendicular to the film plane. Each time when the bottom of a subband approaches the Fermi energy, there is an enhancement of superconductivity referred to as the superconducting shape resonance.[14,17,19,20] Due to a sequence of shape resonances (sequence of QWS), any superconducting property exhibits the thickness-dependent (quantum-size) oscillations.

However, the above picture holds only for systems with an atomically uniform thickness, like recently investigated P*b* nanofilms[15,16,17,19] or perfect tin whiskers.[43] In the presence of inevitable thickness variations in polycrystalline samples, quantum-size oscillations are averaged out. As the system of interest consists of well connected atomically flat superconducting islands (crystallites) with different thicknesses, we expect that due to proximity effects, islands with resonant thicknesses determine the superconducting properties of the whole system. Thus, the resulting T_c follows (approximately) an envelope of the resonant enhancements. Notice that the density of the shape resonances per unit thickness is π/k_F[19] while the typical variation of the nanofilm thickness is about 1 nm. Estimating the Fermi wavenumber as $\approx 10-20\ \text{nm}^{-1}$,[44,45] one concludes that a polycrystalline sample in our study certainly includes various islands with resonant conditions.

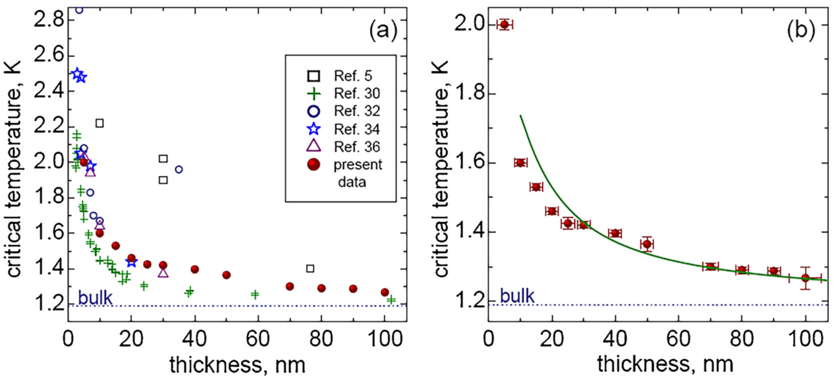

Figure 3. Critical temperature in aluminum superconducting nanofilms versus the nanofilm thickness: (a) the solid circles represent our experimental results, shown together with the previous data from ref. [5] (squares), ref. [30] (crosses), ref. [32] (open circles), ref. [34] (stars), and ref. [36] (triangles, extracted from gap-measurements); (b) the present experimental data in comparison with the theoretical results (solid line) of Equations (5) and (6) calculated, when only the two-leading terms in the $1/d$-expansion of λ_d are taken into account at $\mathcal{A} = 1.16$ nm and $\mathcal{B} = -4.3\ \text{nm}^2$.

To investigate the resonance envelope trend, we invoke the Bogoliubov-de Gennes (BdG) equations that can be written in terms of the subband-dependent excitation gaps Δ_n (chosen real) as[20,46]

$$\Delta_{n'} = \sum_n g_{n'n} \int \frac{\mathrm{d}^2\mathbf{k}}{(2\pi)^2} \frac{\Delta_n}{2E_{n,\mathbf{k}}} \tanh\left(\frac{E_{n,\mathbf{k}}}{2k_\mathrm{B}T}\right) \tag{2}$$

where $n = 1,\ 2,\ 3, \ldots$ enumerates QWS for the electron motion perpendicular to the nanofilm; k is the wave vector for the quasifree in-plane motion of electrons; the quasiparticle energy is given by $E_{n,k} = \sqrt{\xi^2_{n,\mathbf{k}} + \Delta^2_n}$ with the single-particle energy $\xi_{n,\mathbf{k}} = \epsilon_n + \frac{\hbar^2\mathbf{k}^2}{2m} - \mu$ (measured from the chemical potential μ), including the QWS energy $\epsilon_n = \frac{\hbar^2}{2m}\left(\frac{\pi n}{d}\right)^2$. We employ the parabolic band approximation and m is the electron effective mass. The electron-electron interaction strength $g_{n'n}$ in Equation (2) reads[20,46]

$$g_{n'n} = g \int_0^d \mathrm{d}z |\varphi_{n'}(z)|^2 |\varphi_n(z)|^2 = \frac{g}{d}(1 + \delta_{n'n}/2) \tag{3}$$

where $\varphi_n(z) = \sqrt{2/d}\,\sin(\pi nz/d)$ is the QWS wave-function, $\delta_{n'n}$ stands for the discrete delta-function, and g is given by Equation (1).

To find T_c, one should expand the BdG equations in powers of Δ_n and find a linearized (matrix) gap equation, see, for example, ref. [47]. Then, T_c is obtained from the zero-determinant condition for the relevant matrix. As the number of contributing bands is large, so is the rank of the matrix. In general, the equation for T_c can be solved only numerically. However, here we show that, based on previous results of numerically solving the BdG equations, one can find a useful analytical approximation of T_c. Indeed, at resonant thicknesses $\Delta_n \simeq \Delta_{n'}$ for $n \neq n'$.[14,46] Then, T_c can be estimated from

$$1 = \sum_n \frac{g_{n'n} m}{2\pi\hbar^2} \int_{\epsilon_n - \mu}^{+\infty} \mathrm{d}\xi \frac{\theta(\hbar\omega_D - |\xi|)}{2|\xi|} \tanh\left(\frac{|\xi|}{2k_\mathrm{B}T_c}\right) \tag{4}$$

with ω_D being the Debye frequency. At a resonance we have $\mu - \varepsilon_n \gtrsim \hbar\omega_D$, and the number of contributing subbands (i.e., number of QWS below or equal to μ) is estimated as $k_F d/\pi$. Then, Equation (4) is reduced to the effective BCS-like equation

$$\frac{1}{\lambda_d} = \int_0^{\hbar\omega_D} \frac{\mathrm{d}\xi}{\xi} \tanh\left(\frac{\xi}{2k_\mathrm{B}T_c}\right) \tag{5}$$

with the thickness-dependent dimensionless coupling given by the series in powers of 1/d as

$$\lambda_d = \lambda_0\left(1 + \frac{\mathcal{A}}{d} + \frac{\mathcal{B}}{d^2} + \cdots\right) \tag{6}$$

where $\lambda_0 = g_0 N_0$, with $N_0 = mk_F/(2\pi^2\hbar^2)$ the bulk DOS, and

$$\mathcal{A} = \frac{1}{k_F}\left(\frac{\pi}{2} + \frac{g_1}{g_0}\right),\ B = \frac{1}{k_F^2}\left(\frac{\pi g_1}{2g_0} + \frac{g_2}{g_0}\right) \tag{7}$$

To check our approximations, we have compared the solution of Equation (5) with the exact numerical solution of the BdG equations and found only small deviations of about 1–2%.

The conventional approach to treat quantum-size effects in low-dimensional superconductors is based on the thickness-dependent oscillations of DOS due to the appearance of QWS and related multiple subbands, see, for example, ref. [15]. However, from the derivation of Equations (5) and (6) one can see that the electronic DOS contributes only to the factor λ_0 that does not depend on d: in our case the oscillations of DOS do not appear! The thickness dependent terms in λ_d are related to the surface-substrate contributions $g_1/(k_F d)$ and $g_2/(k_F d)^2$ in Equation (1) and to the term $g\delta_{n'n}/(2d)$ in Equation (3). The latter comes from the quantum-confinement modifications of the single-particle wave functions, i.e., it cannot appear for plane waves in a bulk system. We arrive at the important conclusion that in the present case quantum confinement affects T_c only via the modifications of electronic wave functions. As a result, we reveal a subtle interplay of this quantum mechanical effect and the surface-substrate phonon changes, both altering the effective electron-electron attraction. Notice that in addition to the surface-substrate induced changes of the phonon properties, the formation of QWS can also slightly modify the phonon spectrum due to their relations to the mechanical stability.[15] This contribution can be included in g_i ($i = 1, 2, \ldots$), see refs. [46,17,19,20].

For aluminum we have $\lambda_0 = 0.18$.[44] As to g_i ($i = 1, 2, \ldots$), they depend strongly on the fabrication procedure.[17,19,20] In addition, k_F is related to an effective Fermi energy that is used when the BdG equations are taken within the parabolic band approximation and is not precisely known, see discussion in ref. [17]. Furthermore, k_F is shifted up with downsizing in nanoscale superconductors[48] and, strictly speaking, it is also given by a series in powers of $1/d$. Keeping in mind all these complications and uncertainties, it is legitimate to consider the coefficients in λ_d as free parameters known with certain degree of freedom. For illustration, Figure 3(b) shows our theoretical results (solid curve) when the two leading terms in the $1/d$-expansion of λ_d are taken into account. Choosing $\mathcal{A} = 1.16$ nm and $\mathcal{B} = -4.3$ nm^2, we find a good agreement between the experimental (solid circles) and theoretical results for nanofilms with $d \gtrsim 30$ nm. For smaller thicknesses the theory slightly deviates from the experiment. In principle, one can try to add higher order terms in $1/d$, to improve the agreement. However, we recall that our approximations are justified only for sufficiently thick films, see the discussion after Equation (1). In particular, Equation (5) is valid only when $|\mathcal{A}/d|$, $|\mathcal{B}/d^2| \ll 1$. Then, for the chosen values of A and B, one finds the applicability domain of our theoretical study as $d > 10$ nm. The theoretical curve is shown in Figure 3(b) only for thicknesses larger than 10 nm.

Notice that formally using Equations (5) and (6) with a certain adjustment of the free parameters A and B, one can also find a surprisingly good agreement with, for example, the previous data from refs. [5] and [30], see Figure 3(a). However, strictly speaking, Equations (5) and (6) have been derived and justified for the case of almost flat crystallites that are strongly coupled to one another and have the thickness close to d. To microscopically justify a possible general character of Equations (5) and (6), it is mandatory to investigate the quantum-confinement effects in the regime of small crystallites.

Conclusions: We have demonstrated that the quantum confinement in high quality polycrystalline aluminum nanofilms enhances the electron–electron interaction via modifications of electron wave functions. We have derived a useful analytical formula for the electron–electron coupling in the effective BCS-like equation that exhibits interplay between two contributions: one comes from the quantum-confinement modifications of single-particle wave functions and another is related to phonon-spectrum size dependence. Our theoretical results for T_c are in reasonable agreement with our experimental measurements and correlate well with known literature data.

Acknowledgements

Fabrication of samples was done within the joint Russian-Greek Projects No. RFMEFI61717X0001 and No. T4ΔPΩ-00031 “Experimental and theoretical studies of physical properties of low dimensional quantum nanoelectronic systems“. The experimental activity of students EAS, IAG and AAZ was supported by the Russian Science Foundation Grant No. 16-12-10521. Experiments performed by VVZ were supported by the project T3-93 “Quantum solid state systems“ within the framework of the Basic Research Program at the National Research University Higher School of Economics (HSE) and supported by the Russian Academic Excellence Project 5-100.

Conflict of Interest

The authors declare no conflict of interest.

Keywords

nanofilms, quantum-size effects, superconductivity

Received: June 29, 2018
Revised: October 17, 2018
Published online:

[1] K. Yu. Arutyunov, D. S. Golubev, A. D. Zaikin, *Phys. Rep.* **2008**, *464*, 1.
[2] V. Z. Kresin, S. A. Wolf, *Rev. Mod. Phys.* **2009**, *81*, 481.
[3] L. P. Gor’kov, V. Z. Kresin, *Rev. Mod. Phys.* **2018**, *90*, 011001.
[4] H. Alloul, J. Bobroff, M. Gabay, P. J. Hirschfeld, *Rev. Mod. Phys.* **2009**, *81*, 45.
[5] M. Strongin, O. F. Kammerer, A. Paskin, *Phys. Rev. Lett.* **1965**, *14*, 949.
[6] B. Abeles, R. W. Cohen, G. W. Cullen, *Phys. Rev. Lett.* **1966**, *17*, 632.
[7] D. G. Naugle, J. W. Baker, R. E. Allen, *Phys. Rev. B* **1973**, *7*, 3028.
[8] M. Strongin, R. S. Thompson, O. F. Krammerer, J. E. Crow, *Phys. Rev. B* **1970**, *1*, 1078.
[9] R. C. Dynes, J. P. Garno, J. M. Rowell, *Phys. Rev. Lett.* **1978**, *40*, 479.
[10] A. E. White, R. C. Dynes, J. P. Garno, *Phys. Rev. B* **1986**, *33*, R3549.
[11] H. M. Jaeger, D. B. Haviland, B. G. Orr, A. M. Goldman, *Phys. Rev. B* **1989**, *40*, 182.
[12] Y. Liu, K. A. McGreer, B. Nease, D. B. Haviland, G. Martinez, J. W. Halley, A. M. Goldman, *Phys. Rev. Lett.* **1991**, *67*, 2068.
[13] Y. Oreg, A. M. Finkelstein, *Phys. Rev. Lett.* **1999**, *83*, 191.
[14] J. M. Blatt, C. J. Thompson, *Phys. Rev. Lett.* **1963**, *10*, 332.
[15] Y. Guo, Y.-F. Zhang, X.-Y. Bao, T.-Z. Han, Z. Tang, L.-X. Zhang, W.-G. Zhu, E. G. Wang, Q. Niu, Z. Q. Qiu, J.-F. Jia, Z.-X. Zhao, Q.-K. Xue, *Science* **2004**, *306*, 1915.
[16] D. Eom, S. Qin, M.-Y. Chou, C. K. Shih, *Phys. Rev. Lett.* **2006**, *96*, 027005.
[17] A. A. Shanenko, M. D. Croitoru, F. M. Peeters, *Europhys. Lett.* **2006**, *76*, 498.
[18] M. M. Özer, Y. Jia, Z. Zhang, J. R. Thompson, H. H. Weitering, *Science* **2007**, *316*, 1594.
[19] A. A. Shanenko, M. D. Croitoru, F. M. Peeters, *Phys. Rev. B* **2007**, *75*, 014519.
[20] Y. Chen, A. A. Shanenko, F. M. Peeters, *Phys. Rev. B* **2012**, *85*, 224517.
[21] W. Zhao, Q. Wang, M. Liu, W. Zhang, Y. Wang, M. Chen, Y. Guo, K. Hea, X. Chen, Y. Wang, J. Wang, X. Xie, Q. Niu, L. Wang, X. Maa, J. K. Jain, M. H. W. Chan, Q.-K. Xue, *Solid State. Comm.* **2013**, *165*, 59.
[22] Q.-Y. Wang, Z. Li, W.-H. Zhang, Z.-C. Zhang, J.-S. Zhang, W. Li, H. Ding, Y.-B. Ou, P. Deng, K. Chang, J. Wen, C.-L. Song, K. He, J.-F. Jia, S.-H. Ji, Y.-Y. Wang, L.-L. Wang, X. Chen, X.-C. Ma, Q.-K. Xue, *Chin. Phys. Lett.* **2012**, *29*, 037402.
[23] D. Liu, W. Zhang, D. Mou, J. He, Y.-B. Ou, Q.-Y. Wang, Z. Li, L. Wang, L. Zhao, S. He, Y. Peng, X. Liu, C. Chen, L. Yu, G. Liu, X. Dong, J. Zhang, C. Chen, Z. Xu, J. Hu, X. Chen, X. Ma, Q. Xue, X. J. Zhou, *Nature Commun.* **2012**, *3*, 931.
[24] J.-F. Ge, Z.-L. Liu, C. Liu, C.-L. Gao, D. Qian, Q.-K. Xue, Y. Liu, J.-F. Jia, *Nature Mater.* **2015**, *14*, 285.
[25] J. J. Lee, F. T. Schmitt, R. G. Moore, S. Johnston, Y.-T. Cui, W. Li, M. Yi, Z. K. Liu, M. Hashimoto, Y. Zhang, D. H. Lu, T. P. Devereaux, D.-H. Lee, Z.-X. Shen, *Nature* **2014**, *515*, 245.
[26] L. Rademaker, Y. Wang, T. Berlijn, S. Johnston, *New J. Phys.* **2016**, *18*, 022001.
[27] M. D. Croitoru, A. A. Shanenko, A. Vagov, M. V. Milošević, V. M. Axt, F. M. Peeters, *Sci. Rep.* **2015**, *5*, 16515.
[28] M. D. Croitoru, A. A. Shanenko, A. Vagov, A. S. Vasenko, M. V. Milošević, V. M. Axt, F. M. Peeters, *J. Supercond. Nov. Magn.* **2016**, *26*, 605.
[29] I. S. Khukhareva, *Sov. Phys. JETP* **1963**, *16*, 828.
[30] P. N. Chubov, V. V. Eremenko, Yu. A. Pilipenko, *Sov. Phys. JETP* **1969**, *28*, 369.
[31] R. W. Cohen, B. Abeles, *Phys. Rev.* **1968**, *168*, 444.
[32] O. A. E. Cherney, J. Shevchun, *Can. J. Phys.* **1969**, *47*, 1101.
[33] R. V. D’Aiello, S. J. Freedman, *J. Appl. Phys.* **1969**, *40*, 2156.
[34] R. Meservey, P. M. Tedrow, *J. Appl. Phys.* **1971**, *42*, 51.
[35] R. B. Pettit, *Phys. Rev. B* **1976**, *13*, 2865.
[36] N. A. Court, A. J. Ferguson, R. G. Clark, *Supercond. Sci. Technol.* **2008**, *21*, 015013.
[37] M. Zgirski, K. P. Riikonen, V. Tuboltsev, K. Arutyunov, *Nano Lett.* **2005**, *5*, 1029.
[38] M. Zgirski, K. Yu. Arutyunov, *Phys. Rev. B* **2007**, *75*, 172509.
[39] M. Zgirski, K. Yu. Arutyunov, *Physica E* **2007**, *40*, 160.
[40] M. Zgirski, K.-P. Riikonen, V. Touboltsev, K. Yu. Arutyunov, *Phys. Rev. B* **2008**, *77*, 054508.
[41] P. Jalkanen, V. Tuboltsev, A. Virtanen, K. Yu. Arutyunov, J. Räisänen, O. Lebedev, G. Van Tendeloo, *Solid State Commun.* **2007**, *142*, 407.
[42] V. V. Zavyalov, S. A. Chernyaev, K. V. Shein, A. G. Shukaleva, K. Yu. Arutyunov, *J. Phys.: Conf. Ser* **2018**, *969*, 012086.
[43] Yu. Arutyunov, T. V. Ryynanen, J. P. Pekola, A. B. Pavolotski, *Phys. Rev. B* **2001**, *63*, 092506.
[44] P. G. de Gennes, *Superconductivity of Metals and Alloys*. Benjamin, New York, USA **1966**.
[45] J. B. Ketterson, S. N. Song, *Superconductivity*. Cambridge University Press, Cambridge, UK **1999**.
[46] A. A. Shanenko, M. D. Croitoru, F. M. Peeters, *Phys. Rev. B* **2008**, *78*, 054505.
[47] A. A. Shanenko, J. Albino Aguiar, A. Vagov, M. D. Croitoru, M. V. Milošević, *Supercond. Sci. Technol.* **2015**, *28*, 054001.
[48] A. A. Shanenko, M. D. Croitoru, *Phys. Rev. B* **2006**, *73*, 012510.